Available online at www.sciencedirect.com
SCIENCE DIRECT®
Journal of Power Sources 134 (2004) 211–221
JOURNAL OF POWER SOURCES
www.elsevier.com/locate/jpowsour

Charge–discharge characteristics of $LiCoO_2$/mesocarbon microbeads battery with poly(vinyl chloride)-based composite polymer electrolyte

R.H.Y. Subban [a], A.K. Arof [b,*]

[a] *Faculty of Applied Science, MARA University of Technology, 40500 Shah Alam, Selangor, Malaysia*
[b] *Department of Physics, Faculty of Science, University of Malaya, 50603 Kuala Lumpur, Malaysia*

Received 13 January 2004; accepted 22 March 2004

Available online 17 June 2004

Abstract

Polyvinyl chloride (PVC)-based composite polymer electrolyte films consisting of PVC–$LiCF_3SO_3$–SiO_2 are prepared by the solution-casting method. The electrical properties of the electrolyte are investigated for ionic conductivity and its dependence on temperature. The electrolyte with the highest ionic conductivity is used to fabricate a $LiCoO_2$/PVC–$LiCF_3SO_3$–SiO_2/mesocarbon microbeads (MCMB) battery. The charge–discharge characteristics and performance of the battery at room temperature are evaluated to ascertain the effective viability, of these solid electrolytes in lithium-polymer batteries. Battery performances is also investigated at 313, 323 and 333 K.

Keywords: Poly(vinyl chloride); Composite polymer electrolyte; Ionic conductivity; Lithium battery

1. Introduction

The research into lithium batteries, which began in the 1950s, has led to the present rechargeable lithium-ion batteries (LIB) [1,2]. Since then, the industry has evolved to develop lithium-polymer batteries (LPBs) which includes that advanced by Bellcore [3]. In meeting the demands of consumer electronic products, the battery industry has produced cells with higher specific energy and longer cycle-life. As a result, porous polymer, homogeneous polymer and modified lithium-ion batteries have been assembled, mainly by modifying the technology involved in the battery fabrication processes.

The compound $LiCoO_2$ has been investigated as a positive-electrode (cathode) material for use in most of these batteries since the late 1970s when the lithium-polymer batteries were developed [4]. This material is air and water stable with a specific capacity of 140 mAh g^{-1} [5], and has a potential of about 4 V with respect to lithium. Due to the toxicity of cobalt and the scarcity of cobalt sources, however, alternative cathode materials have been developed. This includes other transition metal oxides such as $LiNiO_2$ [5,6] and $LiMn_2O_4$ [5,7–10], and doped transition metal oxides such as $LiNiCoO_2$ [11].

In the case of the negative electrode (anode), carbon (graphite) has been exclusively used. The choice is quite limited due to the requirement of a layered structure for the insertion and de-insertion of lithium ions. Modification of the structure of the carbon anode has led to the use of hard carbon and soft carbon. More recently, nanoscale lithium alloys, such as LiSn, LiAl, LiSi, LiC, and lithium transition metal nitrides, such as LiCoN, have been used as anodes and found to exhibit advantageous features [11].

The present study examine the basic characteristics and cycling performance of a $LiCoO_2$/PVC–$LiCF_3SO_3$–SiO_2/mesocarbon microbeads (MCMB) battery (MCMB: mesocarbon microbeads). The charge–discharge characteristics of the battery have been studied at room temperature, as well as at 313, 323 and 333 K. Prior to fabricating the battery, the electrolyte is characterised by measuring the ionic conductivity and its dependence on temperature. The electrolyte is a composite polymer electrolyte based on poly(vinyl chloride) (PVC) with $LiCF_3SO_3$ as the salt and an organic filler, SiO_2. Most PVC-based electrolytes are of the gel type and only a few batteries based on them have been reported [12–17]. Although PVC-based composite electrolytes have been investigated [18], to the best of our knowledge there have been no studies of PVC-based composite polymer electrolyte systems. A comparison has also been made of some of the characteristics of the batteries fabricated in this work and those of other batteries.

* Corresponding author. Tel.: +60-3-7964-4085; fax: +60-3-7964-4146.
E-mail address: akarof@um.edu.my (A.K. Arof).

0378-7753/$ – see front matter © 2004 Elsevier B.V. All rights reserved.
doi:10.1016/j.jpowsour.2004.03.048

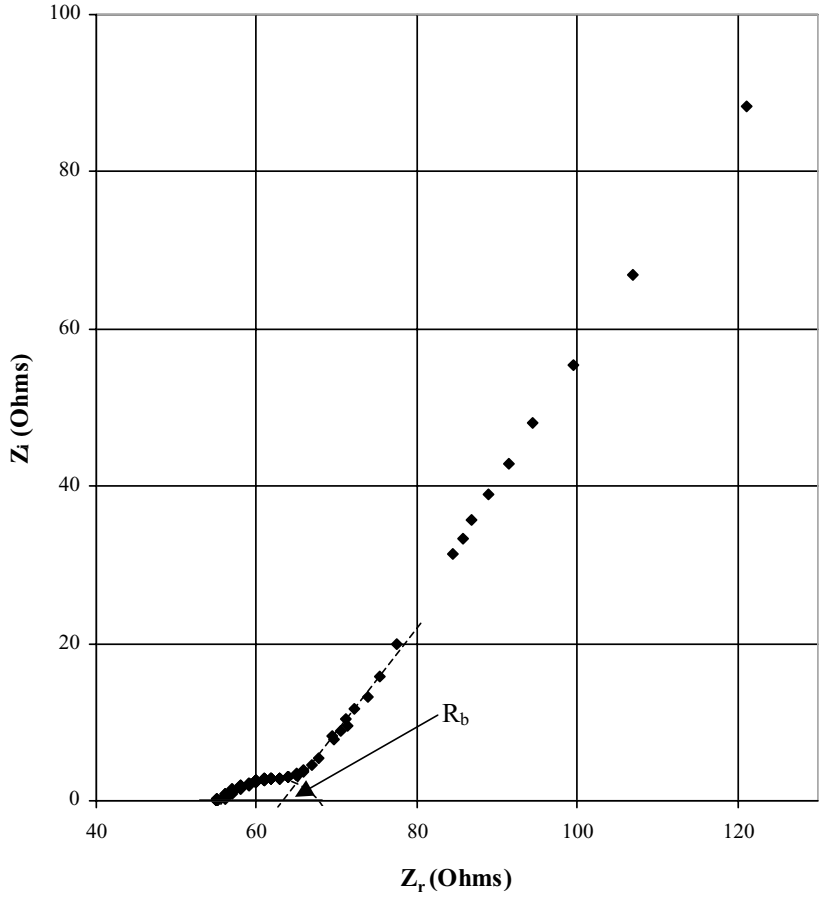

Fig. 1. Complex impedance plot of PVC (33.2%)–$LiCF_3SO_3$ (61.8%)–SiO_2 (5%) polymer electrolyte.

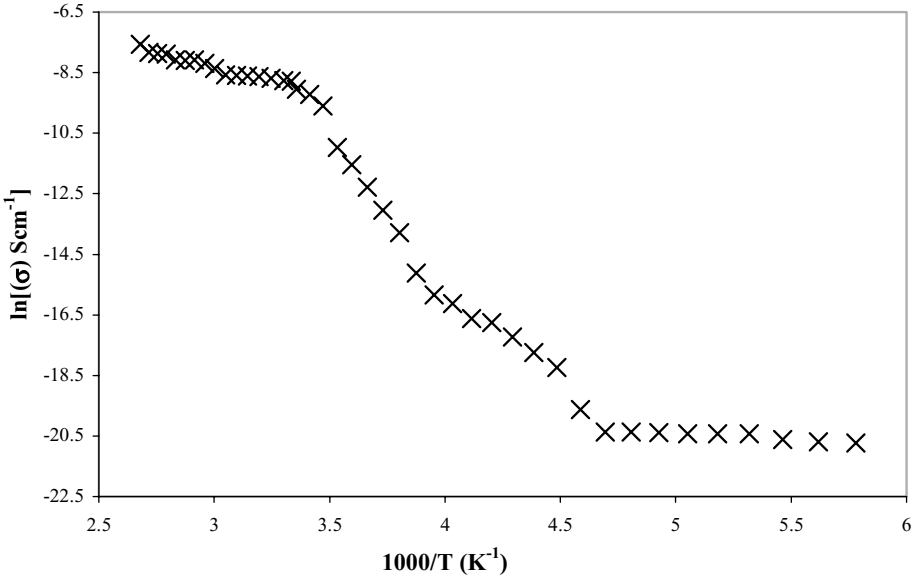

Fig. 2. Arrhenius plot of PVC (33.2%)–$LiCF_3SO_3$ (61.8%)–SiO_2 (5%) polymer electrolyte.

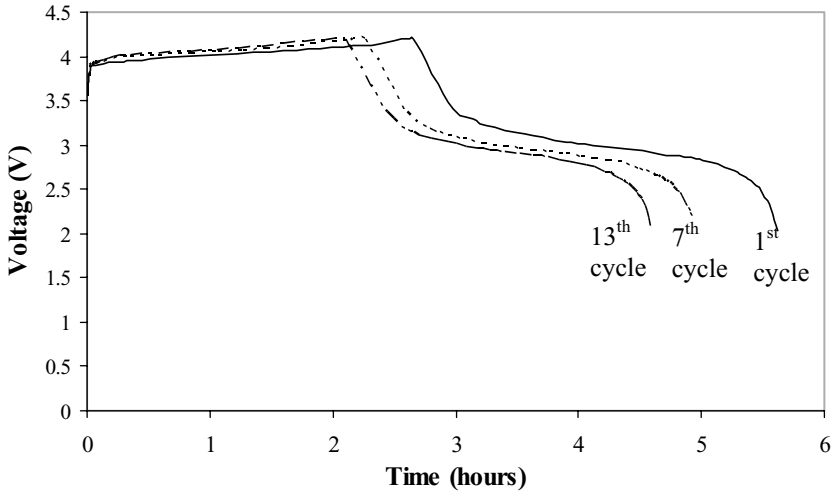

Fig. 3. Discharge curves of $LiCoO_2$/PVC–$LiCF_3SO_3$–SiO_2/MCMB cell at 150 mA for first, seventh and 13th cycle.

2. Experimental

2.1. Synthesis of composite polymer electrolyte

Lithium triflate ($LiCF_3SO_3$) and poly(vinyl chloride) were dissolved separately in tetrahydrofuran (THF) until complete dissolution had taken place. Appropriate amounts of the organic filler, SiO_2 (fumed silica), were then added and stirred until the mixture appeared to be homogeneous. The mixture was then cast into different glass dishes and left to dry by evaporation at room temperature. The films were then removed from the glass dishes and stored in air in a dessicator until required. The PVC was obtained from Sigma, the $LiCF_3SO_3$ from Aldrich, Chemie, and the THF from J.T. Baker.

2.2. Impedance spectroscopy

Complex-impedance measurements were carried out using a computer-controlled HIOKI LCR Hi-tester over frequencies from 40 Hz to 1000 kHz. The dependence of conductivity on temperature was investigated for the highest conducting film at temperatures from 173 to 373 K.

2.3. Preparation of electrodes

Composite cathodes were prepared at room temperature by adding appropriate amounts of $LiCoO_2$, activated carbon and suitable resins to form a homogeneous slurry by mixing in a solvent. The slurry was cast on to an aluminium grid for use as the battery cathode. A similar procedure was used for

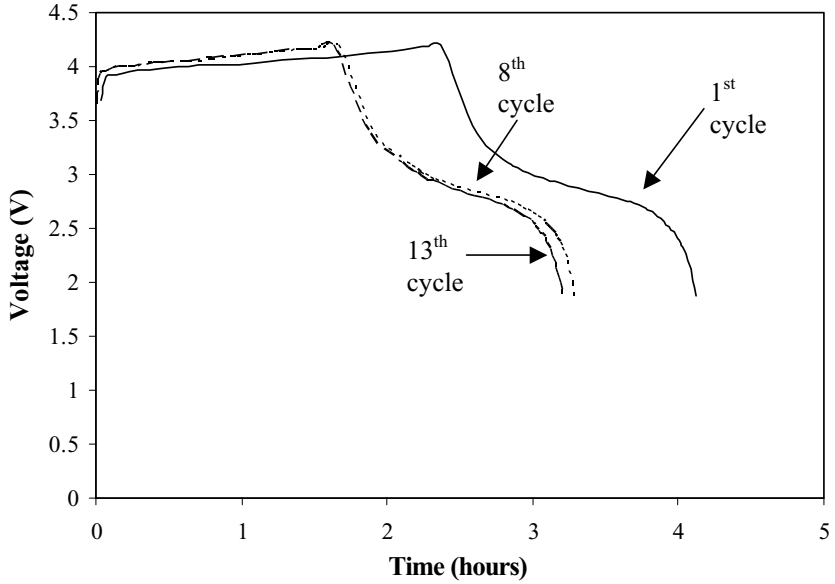

Fig. 4. Discharge curves of $LiCoO_2$/PVC–$LiCF_3SO_3$–SiO_2/MCMB cell at 200 mA for first, eighth and 15th cycle.

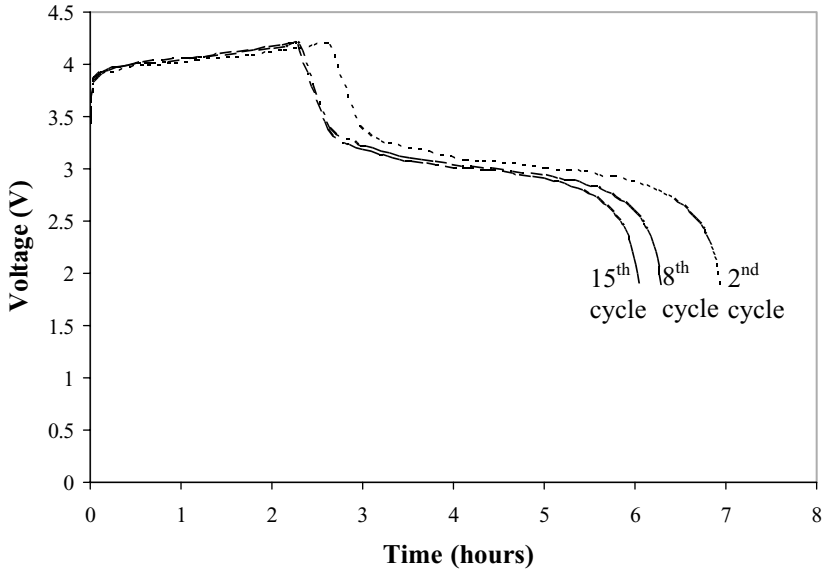

Fig. 5. Discharge curves of $LiCoO_2$/PVC–$LiCF_3SO_3$–SiO_2/MCMB cell at 100 mA for second, eighth and 15th cycle.

the preparation of the composite anode, which consisted of a mixture of mesocarbon microbeads, activated carbon, and suitable resins. The anode materials were mixed and cast on to a copper grid.

2.4. Fabrication of battery

The polymer electrolyte film with the highest conductivity at room temperature was used as the separator for the fabrication of a PVC-based, lithium-polymer secondary battery. The electrodes were cut into dimensions of 3.0 cm × 5.0 cm before stacking with the electrolyte in between. The whole assembly was packed in an aluminium-laminated envelope and sealed in a glovebox.

2.5. Battery characterisation

The battery $LiCoO_2$/PVC–$LiCF_3SO_3$–SiO_2/MCMB was subjected to conditioning for 1 cycle by charging to 4.2 V and discharging to 2.0 V. This was done to stabilize the active materials of the battery by the formation of a solid electrolyte interface (SEI) with even thickness [19]. After conditioning, the battery was tested by measuring its rate discharge. In this test, the battery was charged at 150 mA until it reached a voltage of 4.2 V and then discharged at 150 mA to a cut-off voltage of 2.0 V. The same charging and discharging rate were used for the first test in order to ensure high coulombic efficiency [20]. This was then followed by discharge at 50, 100 and 200 mA. Temperature-dependence studies were also conducted on the battery and were recorded

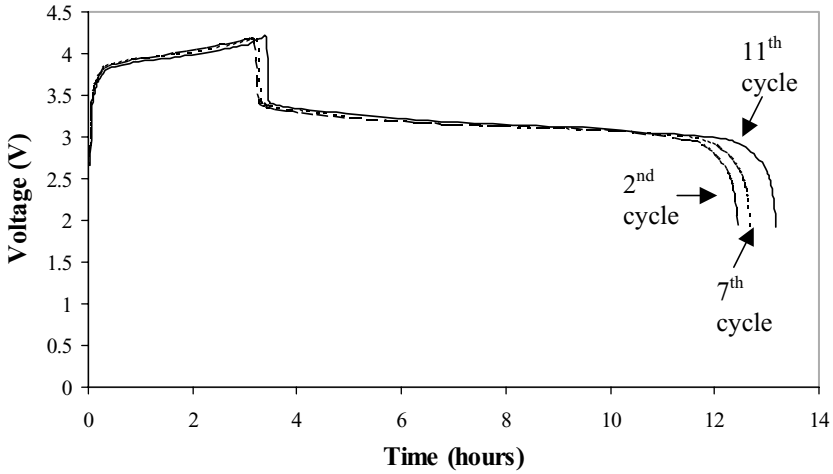

Fig. 6. Discharge curves of $LiCoO_2$/PVC–$LiCF_3SO_3$–SiO_2/MCMB cell at 50 mA for second, seventh and 11th cycle.

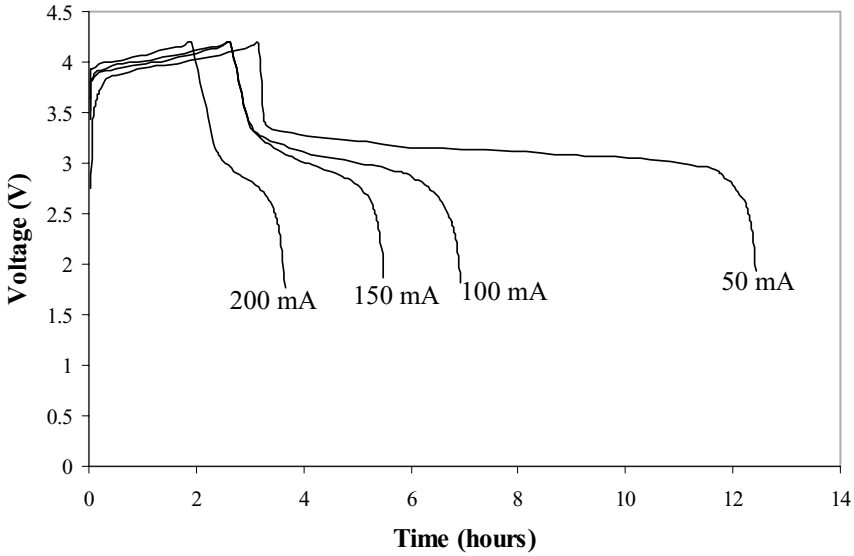

Fig. 7. Discharge characteristics of $LiCoO_2$/PVC–$LiCF_3SO_3$–SiO_2/MCMB cell at 50, 100, 150, and 200 mA.

at temperatures of 313, 323 and 333 K. In those studies, the battery was charged at 150 mA up to 4.2 V at room temperature and stored for 4 h in a temperature chamber before discharge at 50 mA to a voltage of 2.0 V. The conditioning and cycling tests were performed by means of a battery cycler manufactured by Arbin.

3. Results and discussion

3.1. Ionic conductivity of PVC-based polymer electrolyte

The electrical conductivity of the PVC-based polymer electrolyte was highest for a sample with a configuration of 33.2 wt.% PVC, 61.8 wt.% $LiCF_3SO_3$ and 5 wt.% SiO_2.The value was 1.15×10^{-4} S cm^{-1}, and was obtained by substituting the value for R_b into the equation

$$\sigma = \frac{l}{(R_b A)} \quad (1)$$

where l is the thickness of the electrolyte, A the area of cross-section of the electrolyte; and R_b is obtained from the complex impedance plot shown in Fig. 1. The ionic conductivity of the electrolyte is around 0.1 mS cm^{-1}, which is suitable for battery applications [21] and is comparable with electrolytes commonly used in the fabrication of lithium-polymer batteries [15,16,22,23].

The ln(σ) versus 1000/T plot for the polymer electrolyte is given in Fig. 2. This is characteristically Arrhenius in behaviour and therefore indicates that the conductivity of the polymer electrolyte is thermally activated. Thus, the conductivity increases as the temperature is increased. Regression and activation energy values in the range of temperatures studied in this work, are listed in Table 1.

3.2. Battery charge–discharge characteristics

Voltage profiles for the charge–discharge cycles of a $LiCoO_2$/PVC–$LiCF_3SO_3$–SiO_2/MCMB battery at room temperature for discharge currents of 150, 200, 100 and 50 mA are given in Figs. 3–6, respectively. For comparative purpose, the voltage profiles are presented together in Fig. 7. The voltage drop during the initial discharge is higher when the discharge current is increased, and the discharge time increases as the discharge current decreases. The discharge capacity is also higher at lower discharge currents.

The discharge capacity as a function of cycle number for all discharge currents is shown in Fig. 8. The capacity decreases as the cycle number increases; the average values at 50, 100, 150 and 200 mA are 455, 382, 372 and 290 mAh, respectively. The decrease in capacity as the discharge current increases is normal behaviour for lithium-ion batteries and is caused by the higher degree of overpontential at a higher discharge current [14,24]. According to Kim et al. [25], the reduction in capacity at higher discharge current may be due to an increase in the resistance of the polymer electrolyte which can have a thickness of the order of several hundred micrometres when compared with the thickness of the separator (−25 μm) with liquid electrolyte. Hikmet [26] also observed a decrease in discharge capacity with increase in the discharge rate for a $LiCoO_2$/UHMWPE/graphite, battery, where UHMWPE is ultra high molecular weight poly(ethylene ox-

Table 1
Activation energies and regression values

Temperature range (K)	Activation energy (eV)	Regression
173–213	0.15	0.93
213–300	0.73	0.98
300–373	0.03	0.87

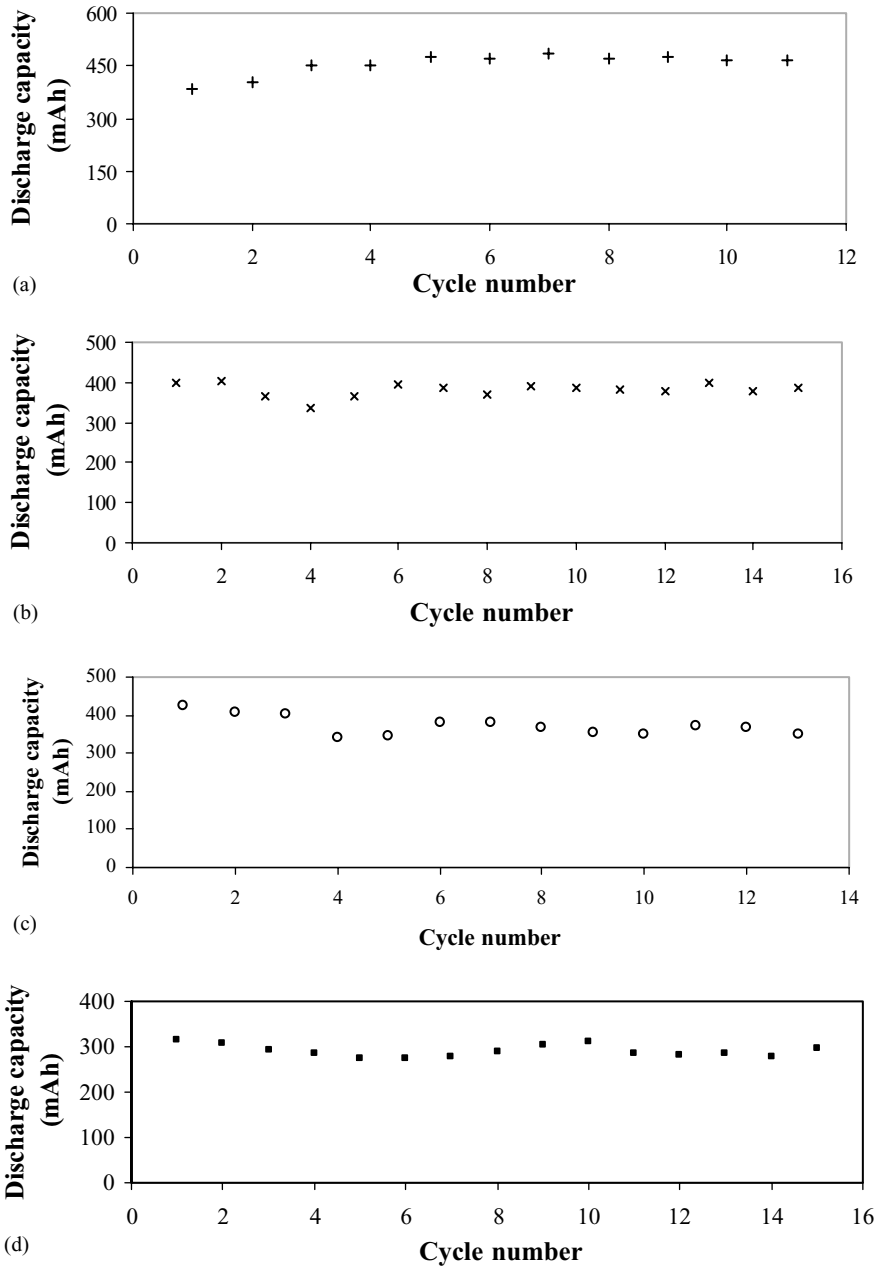

Fig. 8. Discharge capacity as function of cycle number for $LiCoO_2$/PVC–$LiCF_3SO_3$–SiO_2/MCMB cell discharged at (a) 50 (b) 100 (c) 150 and (d) 200 mA.

Table 2
Comparison of PVC-based battery characteristics

Reference	Battery system	OCV (V)	Internal resistance (Ω)	Discharge capacity	Energy density (Jg^{-1})	Power density (wg^{-1})
This work	$LiCoO_2$/PVC–$LiCF_3SO_3$–SiO_2/MCMB	4.2	3.3	118.0 mAh g^{-1} at 150.0 mA (0.25C)	438.0	0.18
[13]	$LiMn_2O_4$/PVC–$LiClO_4$–EC–PC/Li	3.8	–	8.0 mAh at 1.0 mA	–	–
[14]	$LiCoO_2$/PVC–PMMA–$LiPF_6$–EC–DMC/MCMB	4.2	–	111.0 mAh g^{-1} at 2C (90 mA)	–	–
[16]	$LiCoO_2$/PVC–PMMA–SiO_2-$LiClO_4$–EC–DMC/MCMB	4.2	–	120.0 mAh g^{-1} at 1.16 mAcm^{-2} (C/3)	–	–
[17]	Fe–S_2/CI–PVC–$LiClO_4$–PC/Li	–	–	800.0 mAh g^{-1} at 0.1 mA	–	–

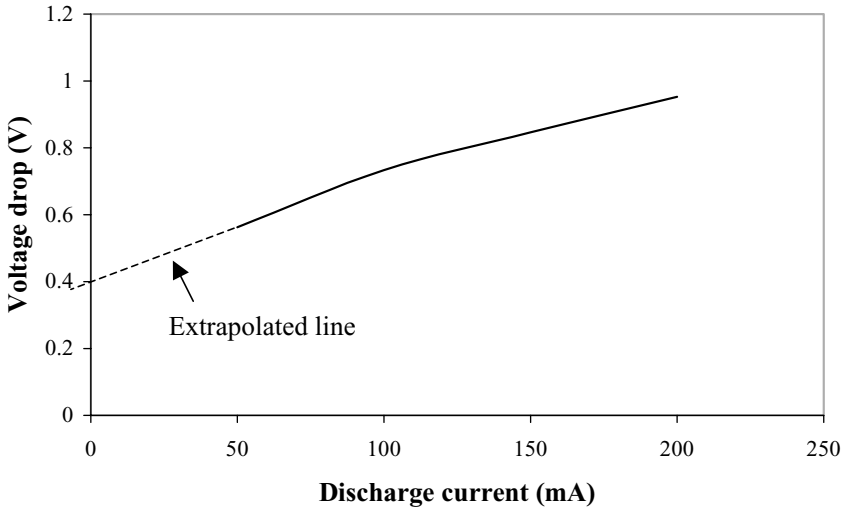

Fig. 9. Voltage drop as function of discharge rate for $LiCoO_2$/PVC–$LiCF_3SO_3$–SiO_2/MCMB cell.

ide). This was attributed to the internal resistance of the battery that is related to the difference between the actual voltage and the open-circuit voltage the so-called 'voltage drop'. The internal resistance of the battery can be estimated from a plot of voltage drop at half discharge capacity against discharge current, as shown in Fig. 9. The relationship is almost linear up to 100 mA and the internal resistance, which is the slope of this part of the plot, is found to be about 3.3 Ω.

The nominal voltage as a function of cycle number for all discharge currents is shown in Fig. 10. The nominal voltage is seen to decrease progressively with cycling. This implies that the interfacial contact between the electrodes and the polymer electrolyte may be deteriorating [27–29]. Such behaviour is caused by a change in the lattice of the cathode-active material during cycling, which degrades the electrical contact between the surfaces of the insertion particles. The deterioration may, in turn, cause the internal resistance of the battery to increase during cycling, particularly for batteries that use a polymer electrolyte with an ionic conductivity of 10^{-4} S cm^{-1} [15,30].

Some characteristics of the battery fabricated in this work are compared with those of other batteries with PVC-based electrolytes and composite polymer systems in Tables 2 and 3, respectively. The capacity of the battery reported in this work is comparable with those of other PVC-based batteries, even when discharged at a high current of 150 mA. Shembel et al. [17] reported a specific capacity of 800 mAh g^{-1} when a cell was discharged at 0.1 mA. The C-rate for the cell reported in [14] is about 46 mAh, hence if the discharge capacity is 11 mAh g^{-1} at 2C rate, the discharge current is about 90 mA. The performance of the cell in the present work is 118 mAh g^{-1} at a discharge current of 150 mA, i.e. better than that in [14], on the other hand, the discharge capacity of the cell in this work is about the same as that reported in [16], but the discharge current is smaller in [16] even for an area of 100 cm^2. With respect to batteries fabricated with other composite polymer systems, it can be observed (Table 3) that the battery in this work has a reasonably good capacity bearing in mind that the measurements were made at room temperature whereas the capacity values of the other batteries were obtained at elevated temperatures.

Temperature dependence studies of the battery are presented in Fig. 11 for the first cycle at temperatures 313,

Table 3
Comparison of characteristics of batteries with composite polymer systems

Reference	Battery system	OCV (V)	Internal resistance (Ω)	Discharge capacity	Energy density (Jg^{-1})	Power density (wg^{-1})
This work	$LiCoO_2$/PVC–$LiCF_3SO_3$–SiO_2/MCMB	4.2	3.3	118.0 mAh g^{-1} at 150 mA (0.25C) (32 °C)	438.0	0.18
[23]	$LiMn_2O_4$/PEO–$LiN(CFSO_2)_2$–Li_2S–B_2S_3/LiC_6	4.5	–	∼0.7 mAh (2C) at 0.1 mA cm^{-2} (0.285 mA)[a] (70 °C)	–	–
[31,32]	$LiNiCoO_2$–Al/PEO–$LiN(CF_3SO_2)_2$–$LiPF_6$-$BaTiO_3$/Li	4.2	–	150.0 mAh g^{-1} at 0.2 mA cm^{-2} (80 °C)	–	–
[33]	$LiFePO_4$–Ag–C/PEO–$LiCF_3SO_3$–ZrO_2/Li	4.2	–	160 mAh g^{-1} at C/5 (100 °C)	–	–

[a] With the understanding that 2.85 cm^2 is the area of the battery.

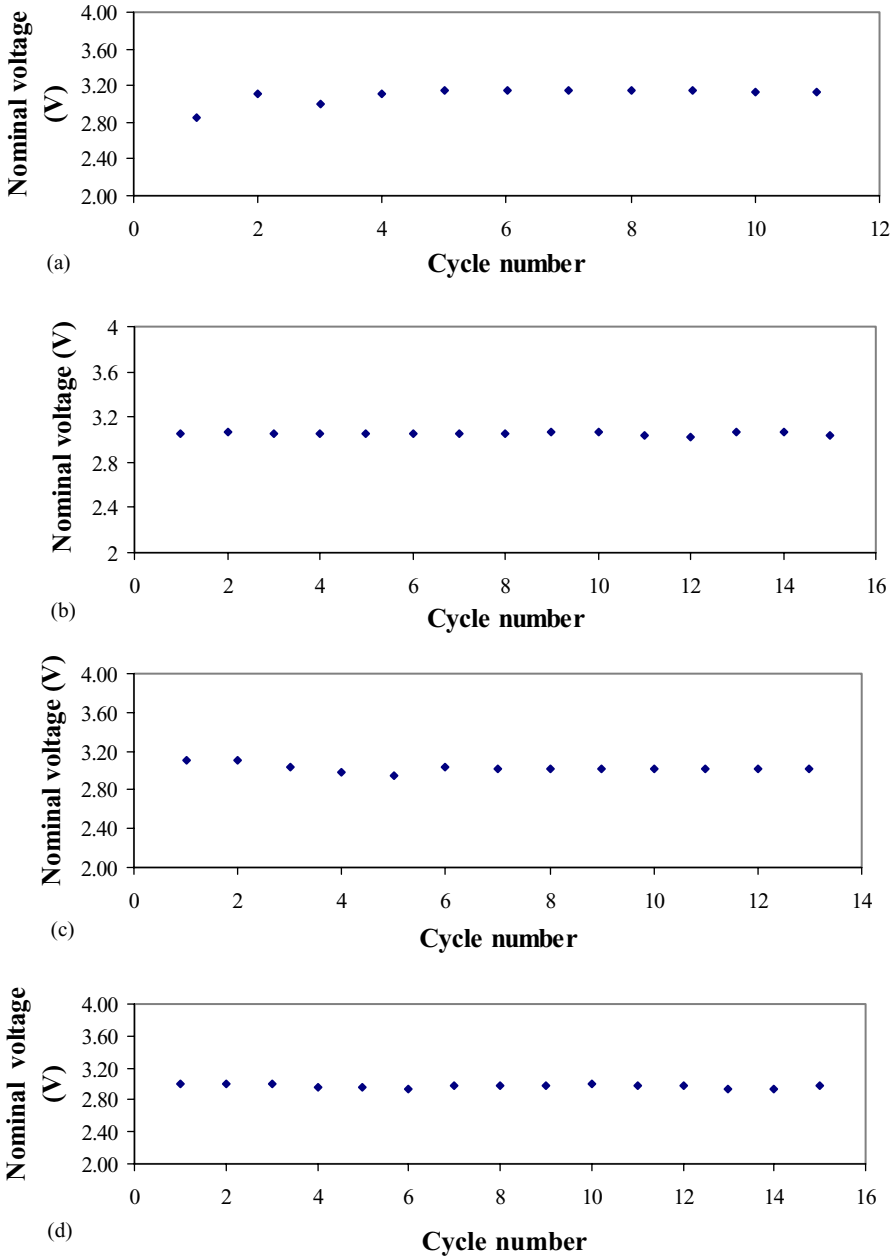

Fig. 10. Nominal voltage as function of cycle number for $LiCoO_2$/PVC–$LiCF_3SO_3$–SiO_2/MCMB cell discharged at (a) 50 (b) 100 (c) 150 and (d) 200 mA.

323 and 333 K. The drop in voltage is smaller as the temperature is increased. At 333 K, the discharge time is much longer, which implies that the discharge capacity is much higher than at 323 and 313 K. These values are calculated and plotted on a graph of capacity versus cycle number, as shown in Fig. 12, and indicate that the battery performance is improved when the temperature is increased. This is consistent with the results obtained from the temperature dependence studies of ionic conductivity. Since the ionic conductivity of the polymer increases with temperature, more ions are available for conduction and thus more ions are able to intercalate and de-intercalate between the two electrodes. Hence, the battery gives a higher discharge capacity at elevated temperatures. An increase in the diffusivity of the lithium ions through the battery when the temperature is increased would also contribute to this improvement.

By taking the discharge characteristic at 333 K as the reference, the percentage capacity can be calculated. A representation of the voltage against percentage discharge capacity is shown in Fig. 13. The graph clearly shows that the discharge capacity decreases as the temperature is decreased. This is substantiated by a plot of percentage capacity against temperature, which is a straight line and therefore indicates that the two quantities are proportional to one another (Fig. 14).

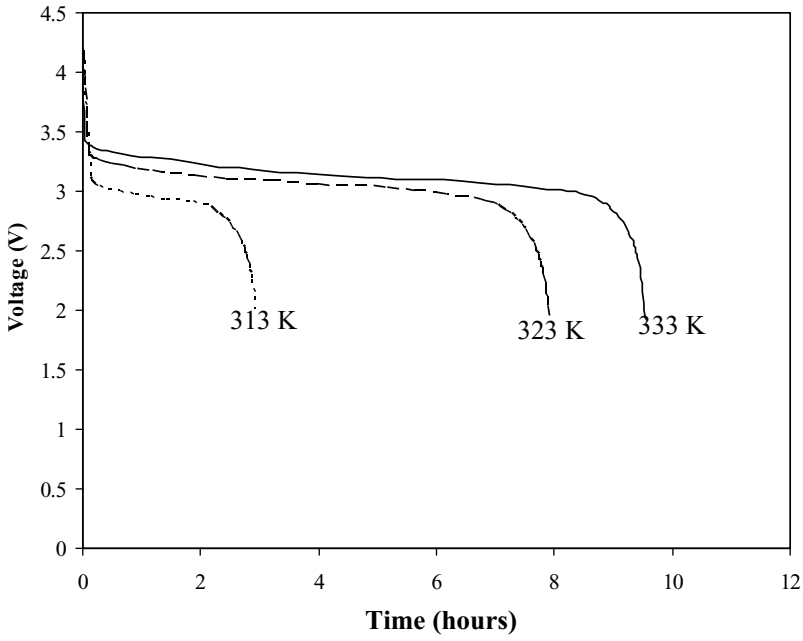

Fig. 11. Discharge characteristics of $LiCoO_2$/PVC–$LiCF_3SO_3$–SiO_2/MCMB cell for first cycle at 313, 323 and 333 K.

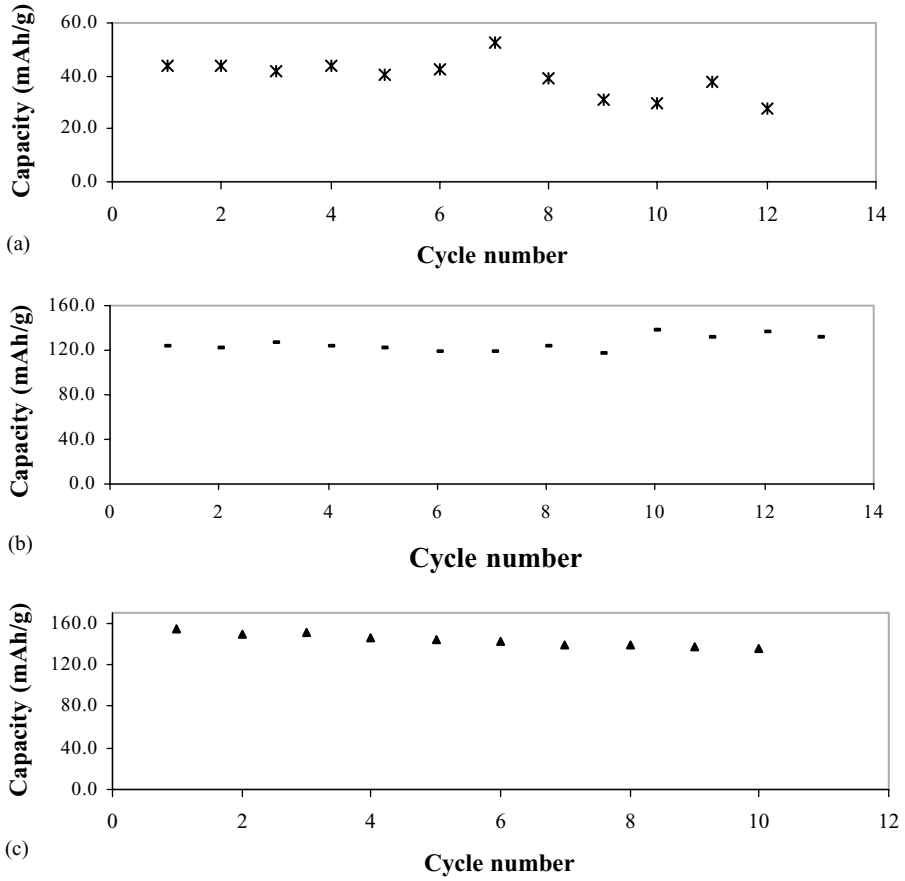

Fig. 12. Discharge capacity as function of cycle number of $LiCoO_2$/PVC–$LiCF_3SO_3$–SiO_2/MCMB cell at (a) 313 (b) 323 and (c) 333 K.

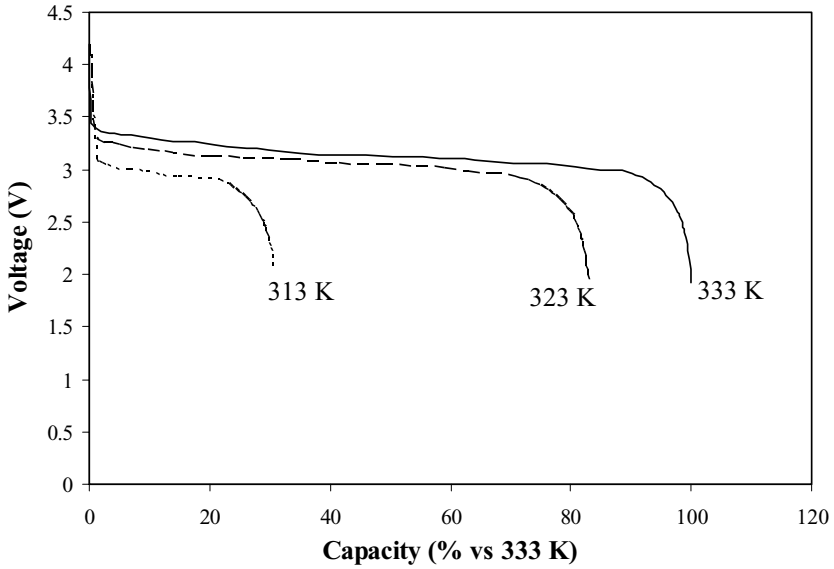

Fig. 13. Rate discharge at 50 mA of $LiCoO_2$/PVC–$LiCF_3SO_3$–SiO_2/MCMB cell at 313, 323 and 333 K.

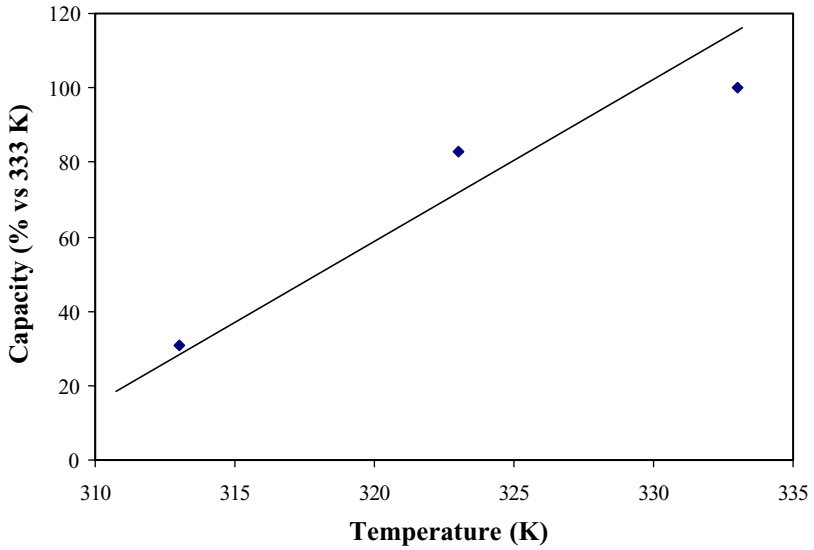

Fig. 14. Capacity–temperature relationship of $LiCoO_2$/PVC–$LiCF_3SO_3$–SiO_2/MCMB battery at different temperatures.

4. Conclusions

A Li^+-ion conducting, PVC-based composite polymer electrolyte with a conductivity of 1.15×10^{-4} S cm^{-1} has been developed and was found to obey the Arrhenius relation. A $LiCoO_2$/PVC–$LiCF_3SO_3$–SiO_2/MCMB battery has demonstrated a room temperature capacity of 118 mAh g^{-1} at a discharge rate of 150 mA in the potential range 2.0–4.2 V. The capacity also increases with temperature.

Acknowledgements

R.H.Y. Subban is grateful to the University Technology MARA for study leave and a scholarship award. The University of Malaya is acknowledged for grant F0191/2002A, and Intran Marketing Sdn. Bhd. is thanked for the loan of the Arbin instrument.

References

[1] M.B. Armand, J.M. Chabagno, M.J. Duclot, in: P. Vasishta, J.N. Mundy, G.K. Shenoy (Eds.), Fast ion Transport in Solids, North Holland, Amsterdam, 1979.
[2] M. Wakihara, O. Yamamoto, Lithium Ion Batteries, Wiley–VCH, Tokyo, 1998.
[3] J.M. Tarascon, A.S. Godtz, C. Schumtz, F. Shokoohi, P.C. Warren, Solid State Ionics 86 (1996) 49.
[4] R. Koksbang, J. Barker, H. Ski, M.Y. Saidi, Solid State Ionics 84 (1996) 1.

[5] D. Rahner, S. Machill, H. Schlorb, K. Siury, M. Klob, W. Plieth, Solid State Ionics 86–88 (1996) 891.
[6] M.S. Whittingham, Solid State Ionics 134 (2000) 169.
[7] M.M. Thackeray, J. Power Sources 97–98 (2001) 7.
[8] P. Endres, B. Fuchs, S. Kemmler Sack, K. Brandt, G. Faust-Becker, H.W. Praas, Solid State Ionics 89 (1996) 221.
[9] T.Y. Shu, F.Z. Yan, Z.L. Qing, C.Z. Ming, D. Li, in: Proceedings of the Solid State Ionics—Materials and Devices, Fuzhou, China, 2000, p. 287.
[10] T. Kanasaku, K. Amezawa, N. Yamamoto, Solid State Ionics 133 (2000) 51.
[11] J. Dahn, in: Proceedings of the Power 2000 Conference, San Diego, 2000.
[12] K.M. Abraham, M. Alamgir, Solid State Ionics 70–71 (1994) 20.
[13] M. Alamgir, K.M. Abraham, J. Power Sources 54 (1995) 40.
[14] H.T. Kim, K.B. Kim, S.W. Kim, J.K. Park, Electrochim. Acta 45 (2000) 4001.
[15] S. Ramesh, A.K. Arof, J. Power Sources 120 (2001) 1.
[16] N.S. Choi, J.K. Park, Electrochim. Acta 46 (2001) 1453.
[17] E.M. Shembel, O.V. Chervakov, L.I. Neduzhko, I.M. Maksyuta, Y.V. Plischuk, D.E. Reisner, P. Novak, D. Meshri, J. Power Sources 96 (2001) 20.
[18] S. Rajendran, T. Uma, Mater. Lett. 44 (2000) 208.
[19] Z. Ogumi, M. Inaba, Bull. Chem. Soc. Jpn. 71 (1998) 521–534.
[20] T. Nagatomo, C. Ichikawa, O. Omoto, J. Electrochem. Soc. 134 (1987) 305–308.
[21] R. Koksbang, I.I. Olsen, D. Shackle, Solid State Ionics 69 (1994) 320.
[22] N. Kamarulzaman, Z. Osman, M.R. Muhamad, Z.A. Ibrahim, A.K. Arof, N.S. Mohamed, J. Power Sources 97–98 (2001) 722.
[23] J. Cho, M. Liu, Electrochim. Acta 42 (1997) 1481.
[24] D.W. Kim, Y.K. Sun, J. Electrochem. Soc. 145 (1998) 1958.
[25] D.W. Kim, J.M. Ko, J.H. Chun, J. Power Sources 93 (2001) 151.
[26] R.A.M. Hikmet, J. Power Sources 92 (2001) 212.
[27] D.W. Kim, Y.K. Sun, J. Power Sources 102 (2001) 41–45.
[28] D.H. Shen, G. Nagasubramanian, C.K. Hung, S. Surampudi, G. Halpert, in: Proceedings of the 182nd Electrochemical Society, Canada, 1992, 261.
[29] D.W. Kim, B. Oh, J.K. Park, Y. K Sun, Solid State Ionics 138 (2000) 41.
[30] K.S. Hwang, T.H. Yoon, C.W. Lee, Y.S. Son, J.K. Hwang, J. Power Sources 75 (1998) 13–18.
[31] Q. Li, T. Itoh, N. Imanishi, A. Hirano, Y. Takeda, O. Yamamoto, Solid State Ionics l59 (2003) 97.
[32] Q. Li, N. Imanishi, A. Hirano, Y. Takeda, O. Yamamoto, J. Power Sources 110 (2002) 38–45.
[33] F.S. Fiory, F. Croce, A. D'Epifanio, S. Licoccia, B. Scrosati, E. Traversa, J. Eur. Ceramic Soc. 24 (6) (2004) 1385–1387.